

UNDERSTANDING THE COOL DA WHITE DWARF PULSATOR, G29–38

S. J. KLEINMAN,^{1,2,3} R. E. NATHER,² D. E. WINGET,^{2,4} J. C. CLEMENS,^{4,5,6} P. A. BRADLEY,⁷ A. KANAAN,^{8,9}
J. L. PROVENCAL,^{10,11} C. F. CLAVER,¹² T. K. WATSON,¹³ K. YANAGIDA,^{2,14} A. NITTA,² J. S. DIXSON,¹⁵
M. A. WOOD,^{16,17} A. D. GRAUER,^{18,19} B. P. HINE,²⁰ G. FONTAINE,^{4,21} JAMES LIEBERT,²²
D. J. SULLIVAN,²³ D. T. WICKRAMASINGHE,²⁴ N. ACHILLEOS,²⁴ T. M. K. MARAR,²⁵
S. SEETHA,²⁵ B. N. ASHOKA,²⁵ E. MEIŠTAS,^{26,27} E. M. LEIBOWITZ,²⁸ P. MOSKALIK,²⁹
J. KRZESIŃSKI,³⁰ J.-E. SOLHEIM,^{27,31} A. BRUVOLD,³¹ D. O'DONOGHUE,³²
D. W. KURTZ,³² B. WARNER,³² PETER MARTINEZ,³² G. VAUCLAIR,³³
N. DOLEZ,³³ M. CHEVRETON,³⁴ M. A. BARSTOW,^{9,35,36}
S. O. KEPLER,⁸ O. GIOVANNINI,^{8,37} T. AUGUSTEIJN,³⁸
C. J. HANSEN,³⁹ AND S. D. KAWALER¹³

Received 1997 March 14; accepted 1997 October 10

ABSTRACT

The white dwarfs are promising laboratories for the study of cosmochronology and stellar evolution. Through observations of the pulsating white dwarfs, we can measure their internal structures and compositions, critical to understanding post-main-sequence evolution, along with their cooling rates, which will allow us to calibrate their ages directly. The most important set of white dwarf variables to measure are the oldest of the pulsators, the cool DA variables (DAVs), which have not been explored previously through asteroseismology due to their complexity and instability. Through a time-series photometry data set spanning 10 yr, we explore the pulsation spectrum of the cool DAV, G29–38 and find an underlying structure of 19 (not including multiplet components) normal-mode, probably $\ell = 1$ pulsations amidst an abundance of time variability and linear combination modes. Modeling results are incomplete, but we suggest possible starting directions and discuss probable values for the stellar mass and hydrogen layer size. For the first time, we have made sense out of the complicated power spectra of a large-amplitude DA pulsator. We have shown that its seemingly erratic set of observed frequencies can be understood in terms of a recurring set of normal-mode pulsations and their linear combinations. With this result, we have opened the interior secrets of the DAVs to future asteroseismological modeling, thereby joining the rest of the known white dwarf pulsators.

Subject headings: stars: individual (G29–38) — stars: oscillations — stars: white dwarfs

1. INTRODUCTION

Because of their status as the end products of most stellar evolution paths, the white dwarfs are among the oldest stars in the galaxy and therefore offer important clues about the universe around us. Studying their interiors will provide solid endpoints for stellar evolution, which will provide insights into nuclear reaction rates, mass loss mechanisms, and basic physical properties of matter in a variety of extreme conditions. Dating the oldest of these stars provides natural constraints on the age of our Galaxy, includ-

ing possible independent measurements of the ages of the disk, the halo, and open and globular clusters.

The key to exploiting the potential of the white dwarfs is buried beneath their relatively thin surface layers: we must discover their internal structure and composition to make them useful. Measuring the ages of the oldest white dwarfs, which have spent only a small fraction of their entire existence *off* the white dwarf cooling track, is as simple as measuring their cooling rates. Theoretical cooling rate models depend on the mass and structure of the white dwarf. Aster-

¹ New Jersey Institute of Technology, Big Bear Solar Observatory, 40386 North Shore Lane, Big Bear City, CA 92314; sjk@begonias.bbso.njit.edu.

² Astronomy Department, University of Texas, Austin, TX 78712.

³ Guest Observer, Mount Stromlo and Siding Spring Observatory, New South Wales, Australia.

⁴ Visiting Astronomer, Canada-France-Hawaii Telescope, operated by the National Research Council of Canada, Centre National de la Recherche Scientifique de France, and the University of Hawaii.

⁵ California Institute of Technology, Pasadena, CA 91125.

⁶ Fairchild Fellow.

⁷ X-2, MS B-220, Los Alamos National Laboratory, Los Alamos, NM 87545.

⁸ Instituto de Física, Universidade Federal do Rio Grande do Sul, 91501-970 Porto Alegre-RS, Brazil.

⁹ Guest Observer, Isaac Newton Telescope, Roque de los Muchachos, La Palma, Canaries.

¹⁰ University of Delaware, Physics and Astronomy Department, Sharp Laboratory, Newark, DE 19716.

¹¹ Guest Observer, Cerro Tololo Inter-American Observatory, Chile.

¹² NOAO, 950 North Cherry Avenue, Tucson, AZ 85726.

¹³ Department of Physics and Astronomy, Iowa State University, Ames, IA 50211.

¹⁴ Current postal address: 5-35-11 Hongōdai, Sakae-ku Yokohama 247, Japan.

¹⁵ M/S ADVP3, DSC Communications Corporation, 1000 Coit Road, Plano, TX 75075.

¹⁶ Department of Physics and Space Sciences, Florida Institute of Technology, 150 West University Boulevard, Melbourne, FL 32901.

¹⁷ Guest Observer, Institute for Astronomy, Honolulu, HI.

¹⁸ Department of Physics and Astronomy, University of Arkansas, Little Rock, AR 72204.

¹⁹ Visiting Astronomer, Kitt Peak National Observatory.

²⁰ NASA Ames Research Center, MS 269-3, Moffett Field, CA 94035.

²¹ Department de Physique, Université de Montréal, C.P. 6128, Montreal, PQ, H3C 3J7 Canada.

oseismology can both determine these physical parameters of a star and provide a means for *directly* measuring a star's cooling rate.

The DAV (or ZZ Ceti) white dwarfs, with hydrogen-dominated spectra, are the coolest ($\approx 13,000$ K) and oldest of the four known classes of white dwarf nonradial g -mode pulsators.⁴⁰ As such, they are the most critical in answering the age question. Unfortunately, they have also proven to be the most difficult to understand.

The techniques of asteroseismology work best when provided with an abundance of stable modes of oscillation. The first white dwarf successfully analyzed, the DOV, PG 1159–035, (Winget et al. 1991) provided over 100 such modes. The best analyzed DBV, GD 358 (Winget et al. 1994), obliged us similarly. Until now, however, the DAVs were not so willing to provide us with the necessary quantity of modes for easy analysis.

The DAVs exhibit distinct trends with temperature: the hotter stars have lower amplitude, shorter period pulsations, and the cooler ones have large-amplitude, longer period pulsations. The hot DAVs have very few modes while the cooler DAVs have many, but most modes are unstable and seem to come and go without forming any obvious patterns of behavior.

In his dissertation, Clemens (1993, 1994) found additional systematic properties in the hotter DAVs by looking at an ensemble of individual pulsators, thereby establishing a technique for applying asteroseismology on these objects that were thought to have too few modes for analysis. He was able to determine the individual properties of each of the hot DAVs he analyzed by seeing how it fitted in with group properties he discovered. In each star he found only a few modes, but when added together, they formed a much larger, coherent set of $\ell = 1$ modes and a few $\ell = 2$ modes.⁴¹ Clemens (1993, 1994) found a successive series of $\ell = 1$ modes from $k = 1$ to $k = 6$ even though no one star had modes at each value of k . Each observed mode, however, was common to more than one star; when a star had an observed mode, it was always in one of the discerned groups.

The implication of this result is that the overall structure of the hot DAVs must be very similar. Comparing the set of observed modes to theoretical models suggests the masses

of the stars Clemens studied are quite near $0.6 M_{\odot}$ and their hydrogen envelopes are near $10^{-4} M_*$ (where M_* is the total mass of the star). The remarkable similarity of the hot DAVs supports the common asteroseismology credo that the pulsators are “otherwise normal stars,” although the cool DAVs with their complex, variable power spectra remained, for the time being, an enigma. The debate over “thick” versus “thin” hydrogen layers, however, is far from over. See for example Fontaine et al. (1994), Fontaine & Wesemael (1997), and recent modeling results from Bradley (1998) for a recent summary.

Here, we present results from an extensive study of one of the cool DAVs, G29–38. We find that although its power spectrum is not stable and changes quite dramatically from one observing season to another (with smaller changes within a season), we can still fit the observed set of pulsation modes with a set of predominantly $\ell = 1$ normal-mode pulsations. The key to this result was two part (1) obtain many seasons of data to observe a larger set of available modes, and (2) accurately identify and separate the linear combinations from the more fundamental modes of oscillation. The linear combinations are observed periodicities whose frequencies are sums and differences of those of other modes; we believe they arise mainly from nonlinear effects in the system.

There has been a great deal of previous interest in G29–38. Its variability was discovered by Shulov & Kopatskaya (1974) and confirmed by McGraw & Robinson (1975). Winget et al. (1990) observed it in 1988 and found a still unexplained phase variation of the dominant oscillation period, but did not explain the bulk of the star's pulsation properties. Zuckerman & Becklin (1987) reported a significant infrared excess in the star at wavelengths longer than $2 \mu\text{m}$, the source of which is also still unknown, although orbiting dust is becoming the consensus (Zuckerman 1993; Koester, Provencal, & Shipman 1997). Barnbaum & Zuckerman (1992) report a possibly periodic radial velocity variation with an unknown source. Kleinman et al. (1994) used the phase timings of a stable pulsation mode at 284 s to place severe limits on what kinds of orbital companions could be included in the system, showing the radial velocity variations cannot be orbital in origin. A recurring thread throughout most of these works

²² Steward Observatory, University of Arizona, Tucson, AZ 85721.

²³ Department of Physics, Victoria University, Box 600, Wellington, New Zealand.

²⁴ Department of Mathematics, Australia National University, Canberra, Australia.

²⁵ Indian Space Research Organization, Bangalore 560 017, India.

²⁶ Institute of Theoretical Physics and Astronomy, Goštauto 12, Vilnius 2600, Lithuania.

²⁷ Guest Observer, Maidanak Observatory, Uzbekistan.

²⁸ Department of Physics and Astronomy, University of Tel Aviv, Ramat Aviv, Tel Aviv 69978, Israel.

²⁹ Copernicus Astronomical Center, Warsaw, Poland.

³⁰ Mount Suhora Observatory, Cracow Pedagogical University, ul. Podchorżych 2, 30-084 Cracow, Poland.

³¹ Institutt for Matematiske Realfag, Universitet i Tromsø, 9000 Tromsø, Norway.

³² Department of Astronomy, University of Cape Town, Rondebosch 7700, Cape Province, South Africa.

³³ Observatoire Midi-Pyrenees, 14 Avenue E. Belin, 31400 Toulouse, France.

³⁴ Observatoire de Paris-Meudon, F-92195 Meudon, Principal Cedex, France.

³⁵ Department of Physics and Astronomy, University of Leicester, Leicester LE1 7RH, UK.

³⁶ PPARC Advanced Fellow.

³⁷ Visiting Astronomer, Laboratorio Nacional de Astrofisica, CNPq, Brazil.

³⁸ European Southern Observatory, Casilla 19001, Santiago 19, Chile.

³⁹ JILA, University of Colorado, Box 440, Boulder, CO 80309.

⁴⁰ The other three classes are the planetary nebula nucleus variables (PNNVs), the DO variables (DOVs), and the DB variables (DBVs). See Brown & Gilliland (1994), for example, for a review of asteroseismology in a broader context.

⁴¹ The surface deformations on a pulsating white dwarf are usually modeled by the set of spherical harmonics, $[Y_{\ell}^m(\theta, \phi)]$ and an additional radial-node index, k . ℓ is the total number of surface nodes and m is the number of surface nodes along a line of longitude. Most observed modes are $\ell = 1$, with a smattering of $\ell = 2$. There have been no reliable identifications of an $\ell = 3$ (or higher) mode in any white dwarf star.

is the variability and complexity of G29–38's power spectra. For the first time, we now propose a simple picture for G29–38's pulsations.

Our results, combined with Clemens's work on the hotter DAVs, place all the DAVs alongside their other pulsating white dwarf cousins and open this crucial class of variables for asteroseismological analysis. We show there is a pattern behind the complex variable nature of these systems and, in the process, discover a different kind of data set is needed to solve these stars. A single set of observations over a single observing season, no matter how well resolved it is, will not suffice. There must be well-sampled observations over many observing seasons.

2. TECHNIQUES

The white dwarfs are particularly rewarding objects for asteroseismology, the gains from which increase with the number of identified modes. (Modes are identified by specifying the values of the three integers, k , ℓ , and m , along with ν or P , the frequency or period.) Cepheids pulsate in one or two observed modes; the δ Scuti star with the most known modes has around 20 (Breger 1995). The white dwarfs, however, can pulsate in hundreds of observable modes. Each normal mode probes a slightly different region of the stellar interior, so having 100 modes is like having 100 probes, all going to different depths and locations in the star's interior.

The advantages of white dwarfs as asteroseismological laboratories quickly become their biggest disadvantage as well: they are very complicated. With so many modes active at the same time, we need extended data sets to be able to resolve and identify closely spaced modes, since the resolution of the Fourier transform (FT), which we use to search for periodicities in our reduced light curves, is proportional to the inverse of the time duration of the light curve. Even with a high-resolution FT, we can still have problems resolving closely spaced modes if the alias peaks caused by observing gaps end up near real modes of the star. The FT finds an inevitable ambiguity in cycle count of each measured frequency due to these gaps. For nightly observations from a single site, we therefore get alias peaks separated from the real ones by integral multiples of 1 cycle day⁻¹. Unfortunately, this is near the typical white dwarf rotation rate that causes *real* modes to be present, separated by ≈ 1 day⁻¹ in frequency.

In order to eliminate these troublesome 1 day⁻¹ aliases, we strive to eliminate the 1 day gap in our data. To do this, we set up a network of collaborating astronomers around the globe, all observing the same star over the same time period with similar tools and observing techniques. This network, called the Whole Earth Telescope (WET; Nather et al. 1990), has been used quite successfully in the study of DO and DB variables. With the WET, we can obtain data uninterrupted by the daily rising of the Sun and hence produce vastly improved FTs, with few aliases surrounding the real peaks.

Armed with a nearly alias-free transform, the goal of asteroseismology is to match each observed frequency with a unique value of k , ℓ , and m . If a full set of modes (say all the possible m values for at least two values of ℓ over a consecutive series of k values) are present in the star, the job is relatively easy. If not, then clues must be taken whenever available and pieced together for a consistent final picture. The clues involve the spacings between modes of same k

and ℓ but different m , and those between modes of same ℓ and m , but different k .

As the number of radial nodes (k) increases, the frequency of a g -mode decreases (there is less of a restoring force since the wavelength of the oscillation decreases, meaning less mass is present to supply the gravitational restoring force). In the asymptotic (high k) limit, the modes with same ℓ are equally spaced in period. The periods P of such modes are given by (see, for example Unno et al. 1989):

$$P = \frac{k \Delta \Pi}{\sqrt{\ell(\ell + 1)}} + \text{constant}, \quad (1)$$

where $\Delta \Pi$ is a constant related to the period spacing and the additive constant is small. $\Delta \Pi$ itself is primarily a function of the mass of the star and is truly constant only for stars of uniform composition. Adding compositionally stratified layers (white dwarf stars have a very high gravity that separates and stratifies the constituent elements), or any other radial discontinuity, to a model star makes the value of $\Delta \Pi$ different for each mode, although the mean remains a good measure of the total stellar mass. The deviations from uniformity of $\Delta \Pi$ measure the layering present in the star. This effect is called mode trapping as modes with nodes near the composition transition boundaries will have their periods shifted slightly so the nodes correspond more closely to the transition discontinuities (Winget, Van Horn, & Hansen 1981; Brassard et al. 1992).

As long as the spherical harmonics are valid representations of the observed surface distortions (they are as valid as our assumption of spherical symmetry), their underlying symmetry implies that the period of each mode depends only on k and ℓ , the total number of surface nodal lines, and not on how the nodes are arranged on the surface (i.e., m). When the underlying symmetry is broken, however, the observed periods become a function of m as well. Rotation breaks the symmetry and splits each mode of a given k and ℓ into a multiplet of modes with $2\ell + 1$ components with m running from $-\ell$ to ℓ .

For slow rotation, the frequency difference ($\Delta\sigma$) for each m mode is given, to first order, by:

$$\Delta\sigma = m(1 - C_{\ell,k})\Omega, \quad (2)$$

where Ω is the constant stellar rotation frequency and $C_{\ell,k}$ is, in general, a complicated function of the star's density and modal displacements that in the asymptotic (large k) limit, approaches the value $1/\ell(\ell + 1)$. Thus, modes of the same k and ℓ but different m will be uniformly spaced in frequency and, barring radially differential rotation, all modes with the same ℓ will have the same frequency spacings. If radially differential rotation, which changes the effective value of Ω for each mode, is present, we will see a corresponding systematic pattern in the m splittings as a function of k . Since the white dwarf rotation periods so far measured with the WET are near 1 day, we expect the $\ell = 1$ m spacing to be on the order of 6 μ Hz, much smaller than the typical period spacing, $\Delta \Pi$, which is close to 150 μ Hz in the region of main power. Since these rotational spacings are small, we expect to find closely spaced triplets for $\ell = 1$ modes and quintuplets for $\ell = 2$.

Having accurately isolated and measured the frequencies of the pulsations with a long time base of observations, we can actually observe stellar evolution in progress. The period of a mode changes slightly as the star cools and/or

contracts. The contraction process (presumably dominating only in the hottest of the pre-white dwarf pulsators, since white dwarfs cool at essentially constant radius) decreases the period with time while cooling increases it. Since the rates of change (or \dot{P} 's) are very small (of order $10^{-15} \text{ s s}^{-1}$ for an average DAV), this is a very difficult measurement, but an extremely important one. Once we can measure the rate at which a star is cooling (Winget et al. 1991; Kepler 1993), we can empirically calibrate the white dwarf cooling curve, and hence the luminosity function (Liebert, Dahn, & Monet 1988) to measure directly the age of the white dwarfs (Winget et al. 1987).

3. OBSERVATIONS

The WET is the ideal tool for analysis of stars with stable pulsation spectra. For most DAVs, however, it is not enough. During any given season of observations, no matter how well resolved the power spectrum of any one star, only a few independent pulsation modes are present; the rest of the frequencies found in the power spectrum are linear combinations of existing modes. If, however, we observe the same star over many seasons, we can add a few new modes each year and slowly build them up to see a larger set of possible modes. This approach will work only if there is a stable underlying pattern to the star's pulsations, that is, if it picks and chooses a few modes each season from a predefined, limited set of possibilities. We found this to be the case with G29–38.

Presented here are over 1100 hours of time-series photometry (we call the technique *temporal spectroscopy*) on G29–38, representing the results of three campaign observations (two WET runs and a double-site venture between SAAO and McDonald) and many years of intense single-site coverage. They span the 10 yr from 1985 to 1994 with data every year except 1986 and 1987. Rather than present the complete lengthy table of observations here, which can be found in its entirety in Kleinman (1995) and nearly complete in Kleinman et al. (1994), we list in Table 1 only the sites and telescopes that have contributed data, and in Table 2 the additional observations used in this work that were not listed in the Kleinman et al. (1994) paper.

The data were all reduced as described in Nather et al. (1990), transforming the raw light curves to extinction-corrected relative-intensity measurements. The raw data consist of either two or three light curves, measuring the

TABLE 1
DATA-PROVIDING SITES

Location	Telescope
CTIO	1.5 m
Itajuba, LNA	1.6 m
KPNO	1.3 m
La Palma (INT)	2.5 m
Maidanak	1.0 m
Mauna Kea (Air Force).....	24"
Mauna Kea (CFHT)	3.6 m
McDonald	30"
McDonald	36"
McDonald	82"
OHP	1.93 m
SAAO	30"
SAAO	40"
SAAO	74"
Siding Spring	24"
Siding Spring	40"

TABLE 2
ADDITIONAL OBSERVATIONS USED IN THIS WORK THAT ARE NOT LISTED
IN KLEINMAN ET AL. 1994

Telescope	Run Name	Date (UT)	Start (UT)
SAAO 74"	s3598	1985 Aug 8	0:54:04
SAAO 74"	s3606	1985 Aug 10	22:23:42
SAAO 30"	s3615	1985 Aug 13	20:56:20
SAAO 30"	s3618	1985 Aug 14	20:23:40
SAAO 30"	s3621	1985 Aug 15	20:24:00
SAAO 30"	s3624	1985 Aug 16	19:51:20
SAAO 30"	s3628	1985 Aug 17	20:14:20
SAAO 30"	s3631	1985 Aug 19	20:42:20
SAAO 40"	s3634	1985 Aug 20	21:05:16
SAAO 40"	s3638	1985 Aug 21	22:21:45
McDonald 36"	r3084	1985 Aug 22	6:37:26
McDonald 36"	r3085	1985 Aug 23	7:43:21
SAAO 40"	s3642	1985 Aug 23	20:54:18
SAAO 40"	s3645	1985 Aug 24	20:59:43
SAAO 40"	s3647	1985 Aug 25	20:06:20
McDonald 36"	r3086	1985 Aug 26	7:19:19
SAAO 40"	s3651	1985 Aug 26	20:20:03
SAAO 30"	s3654	1985 Sep 10	18:44:20
SAAO 30"	s3655	1985 Sep 13	17:42:00
SAAO 30"	s3656	1985 Sep 14	17:43:00
SAAO 30"	s3658	1985 Sep 15	0:42:40
SAAO 30"	s3660	1985 Sep 15	17:39:20
SAAO 30"	s3663	1985 Sep 16	17:39:20
McDonald 82"	r3088	1985 Oct 22	2:58:37
McDonald 82"	r3094	1985 Oct 31	3:02:00
McDonald 82"	r3095	1985 Nov 1	1:56:30
McDonald 36"	sjk-0264	1993 Jul 21	9:16:30
McDonald 36"	tkw-0034	1993 Aug 11	8:23:00
McDonald 36"	tkw-0040	1993 Aug 16	4:16:00
McDonald 36"	sjk-0265	1993 Sep 14	2:04:00
McDonald 36"	sjk-0266	1993 Sep 14	9:24:30
McDonald 36"	sjk-0267	1993 Sep 15	1:53:30
McDonald 36"	sjk-0268	1993 Sep 16	2:03:30
McDonald 36"	sjk-0269	1993 Sep 17	2:34:00
McDonald 82"	sjk-0270	1993 Sep 18	3:52:30
McDonald 82"	sjk-0276	1993 Sep 19	3:39:30
McDonald 82"	sjk-0277	1993 Sep 20	3:39:00
McDonald 82"	sjk-0278	1993 Sep 20	5:05:30
McDonald 82"	sjk-0279	1993 Sep 20	10:32:30
McDonald 82"	sjk-0281	1993 Sep 21	4:38:30
McDonald 36"	sjk-0282	1993 Nov 4	1:11:30
McDonald 36"	sjk-0283	1993 Nov 5	1:12:30
McDonald 36"	sjk-0285	1993 Nov 6	0:54:00
McDonald 36"	sjk-0287	1993 Nov 7	0:55:30
McDonald 36"	sjk-0288	1993 Nov 8	2:17:00
McDonald 36"	sjk-0289	1993 Nov 8	5:45:00
McDonald 36"	sjk-0293	1993 Dec 14	1:57:30
McDonald 36"	sjk-0295	1993 Dec 15	0:38:00
McDonald 36"	sjk-0297	1993 Dec 16	2:05:30
McDonald 36"	sjk-0299	1993 Dec 17	1:01:30
McDonald 36"	sjk-0302	1993 Dec 18	0:49:00
Siding Spring 24"	sjk-0363	1994 May 14	18:44:00
Siding Spring 24"	sjk-0368	1994 May 15	18:44:30
Siding Spring 24"	sjk-0373	1994 May 16	18:43:30

variable star, the comparison star, and in the case of three-channel instruments, the sky as well. With two-channel instruments, we occasionally move the telescope off the target and comparison stars to sample sky. The instruments used for most of these observations are described by Kleinman, Nather, & Phillips (1996).

4. RESULTS

After reducing each data set, typically a week or two in length, we calculated its FT, which is displayed schematically in Figure 1. Each line represents a periodicity identified at that period. Since the dynamic range in the system is

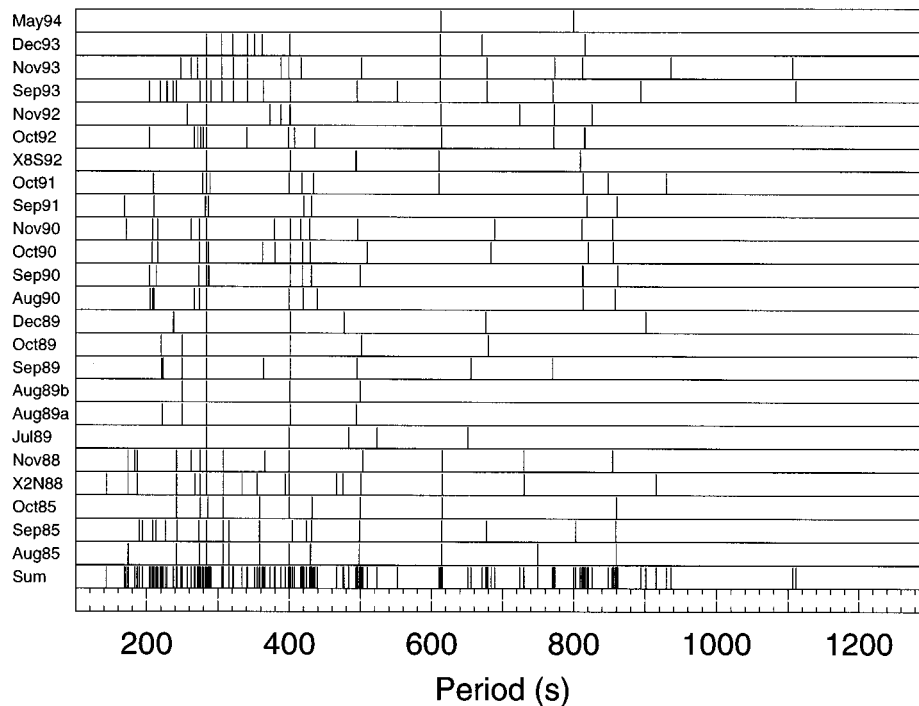


FIG. 1.—Schematic diagram of G29—38's periodicities for the entire data set

large, we have ignored amplitude information and plotted every periodicity with a line of the same height. Each panel is labeled for the month and year of the data, with the exception of X2N88 and X8S92, which are data from the second WET run in 1988 November, and the eighth WET run in 1992 September, respectively. The bottom row of the plot, labeled Sum, contains all the modes in the panels above, collapsed into one.

While there is a wealth of information in this plot, the most striking feature is the near continuum of modes shown in the Sum row in Figure 1. Were all these modes simply $\ell = 1$ and even $\ell = 2$ modes, the mode density would not be nearly so great and there would be distinct gaps between modes.

The most obvious explanation for this result is the known abundance of linear combination frequencies that were not removed in the plot. Our ability to identify (and hence remove) the linear combinations depends greatly on the signal-to-noise ratio and the resolution of each transform. To help avoid uncertain and incorrect identifications, we now restrict the analysis to the best data sets available—one per year: 1985 August, a two-site campaign by South Africa and McDonald; X2N88, the first WET campaign; 1989 September, a 20 night data set from McDonald; 1990 October and 1993 September, slightly smaller single-site data sets from McDonald; and X8S92, the second G29—38 WET campaign.

Identifying the combination frequencies is a difficult task. First, we must identify the three frequencies that form the combination, then decide which are the “real modes” and which is the combination. That is, if we find three signals with frequencies, A, B, and C such that $A + B = C$, we need to decide whether A is the difference frequency of two modes B and C, B is the difference frequency of A and C, or C is the sum frequency of A and B. To identify the combinations, we wrote a simple computer program that goes through a list of identified frequencies from the power

spectra. In developing this code, we found it identified every combination we found by hand, plus a few we did not. In addition, while we often stopped after finding one possible combination that contained a given mode, the computer code found all possible combinations, often finding some more exact than those we had originally identified. The code takes into account possible misidentification of the frequencies if there are dominant aliases present, and applies a selectable equality criteria in determining each match.

Once we had identified the combinations, we decided which were real and which were combinations using the following guidelines: relative mode amplitudes (combinations generally have smaller amplitudes), number of combinations with each mode (combinations with combination modes are less likely than first-order combinations), the existence of multiplet structure (two multiplets added together produce a distinctly different structure in the combination), and the way modes and their combinations disappear and recur in the various data sets (a *parent* mode can appear without its combinations, but not vice versa). Still, though, there were a couple occasions when we could not decide without resort to a model that predicts normal modes. In these cases, we assumed modes with periods near the expected groups were real and not combinations. We will gladly make available the list of frequencies or transforms to anyone who wishes to seriously explore this procedure in more detail. The FTs and mode lists are included in Kleinman (1995) as well.

Figure 2 is the schematic period diagram for this data subset, after removing the identified linear combination frequencies. This new schematic period diagram is substantially cleaner and shows the mode groupings we would expect for normal-mode pulsations. The roughly equally spaced groups seen in the Sum row of Figure 2 suggest a mean period spacing of roughly 50 s, consistent with models of $0.6 M_{\odot}$ DAVs $\ell = 1$ spacings (Bradley 1996). If these are

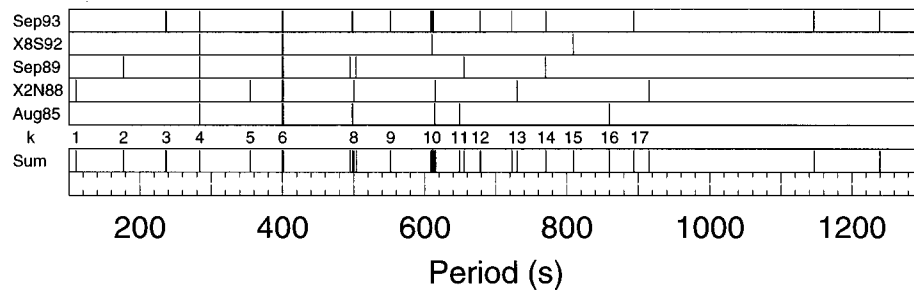


FIG. 2.—Schematic diagram of G29–38's periodicities minus the linear combination modes

all $\ell = 1$ modes, we see a nearly complete set of them from 110 s to 900 s with two more at longer periods. With few exceptions, the groups are tight and have distinct gaps between them.

As Figure 1 readily shows, the power spectrum of G29–38 changes dramatically from year to year. This is even more obvious in Figure 3, which shows a portion of the FT, retaining real amplitudes, for several of our best data sets. G29–38 appears, however, to make its most dramatic changes when the star is behind the Sun and we cannot watch it. (This certainly sets an upper limit on the timescale of change, something that might prove useful once we understand why it makes such drastic changes.) While this predisposition means we do not get to watch the star change, the advantage is that the FT of each individual year provides a relatively stable set of modes that may be used for asteroseismological analysis.

5. MODE DISCUSSION

As discussed earlier, we expect g -modes of identical ℓ values to be equally spaced in period in the asymptotic (high- k) limit. We cannot, however, now go and search for strictly uniform period spacing, because we are *not* in the

asymptotic high- k limit here. We do not expect to find a strictly uniform period spacing since we have identified modes possibly starting at $k = 1$, which is certainly *not* in the high- k limit. Instead, we expect to see significant departures until we get to the higher k modes (our experience shows $k = 10$ is a good rule of thumb). We also expect deviations on the order of 10 s or so due to mode-trapping effects. In some cases, however, models of Bradley (1996) show deviations of as much as 20–30 s.

We tried many different methods to quantitatively search for equal period spacings in this observed set of modes while simultaneously allowing for the inevitable departures from strictly uniform spacing, but did not succeed in finding any significant results. The fault may not, however, be in the data: the same tests failed to find significant period spacings in some of the model-derived test data as well. We therefore believe that the inability to statistically determine a significant mean period spacing does *not* affect (either pro or con) the model of single- ℓ pulsations and continue under the assumption that the approximate equal period spacing seen in these modes is significant and that most likely, these are a series of successive- k , $\ell = 1$ g -modes. While the goal of studying this star, and others like it, must be to uniquely

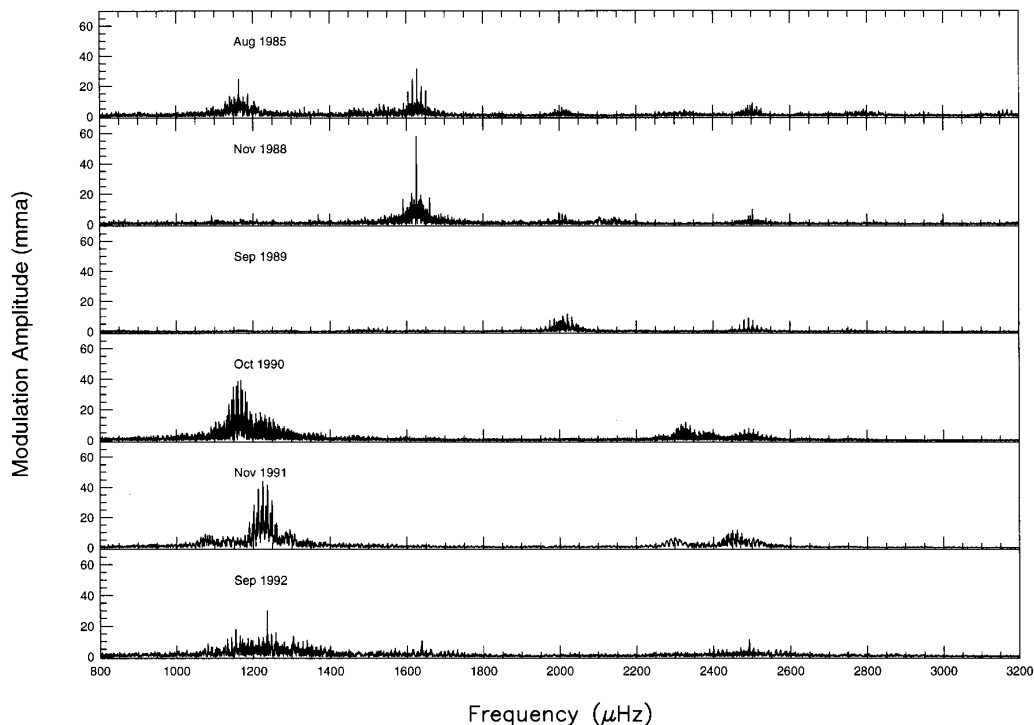


FIG. 3.—Portion of G29–38's FT for several of our best seasons. The large-amplitude changes are obvious.

determine k , ℓ , and m for each mode so we can proceed to explore the white dwarf interiors, were we to go no further in the analysis than where we are now, we could conclude with the discovery of a pattern to G29–38’s seemingly hazardous behavior: *a recurring set of stable modes*. With its now understood wealth of normal-mode oscillations, G29–38 has become the DAV of choice for asteroseismology. We could now commence additional observing programs to help determine ℓ values including perhaps, the spectroscopic methods described by Robinson et al. (1995). In addition, we now know how to make use of the entire set of easy-to-observe, large-amplitude DA pulsators to get a similar set of information.

However, since we are compelled by the observed period spacing, we will continue the analysis under the assumption that each group is a different k , $\ell = 1$ mode. In Figure 2, we provide a running k assignment for each group. We will later discuss the uncertainties of this assignment, but for now, they serve as references to make the ensuing discussion easier.

The data from 1993 September have the most modes and nicely reproduce the ≈ 50 s spacing seen in the Sum row of Figure 2 earlier. This season is unique in that there appear to be six consecutive overtones (k ’s) in one period range. The other seasons also show roughly equally spaced groups, but are often missing one or more k ’s in between each observed mode. The Sum row shows all the gaps (but one) are filled, and we see what appears to be a set of same- ℓ modes from $k = 1$ to $k = 17$. Almost half of the observed modes repeat at least once in the data set, and four are present in four of the five data sets. We now have strong evidence for a series of successive- k , same- ℓ modes.

These same- ℓ modes fit well with an $\ell = 1$ model and its expected period spacing with the possible exceptions of the two modes near $k = 17$, although they could also be $k = 17$ and $k = 18$ without much problem. These two modes, the 894 s mode in 1993 September and the 915 s mode in X2N88, are separated by 21 s, a little too close, but not completely impossible, to be different k ’s (17 and 18), same ℓ pulled closer by mode trapping. Models of Brassard et al. (1992) and Bradley (1993) with hydrogen layer masses near $10^{-10}M_*$ do, for example, show the strong mode trapping this identification implies near these periods, although this match requires a rather limited parameter set. In frequency, the separation is 26 μHz , too large to easily fit the frequency spacings of the known multiplets. We cannot yet completely settle this ambiguity, but are relieved to know it does not affect the rest of the pattern.

5.1. Identification Ambiguities

As the two footnotes in our list of observed periods, Table 3, suggest, there are still some ambiguities in our mode identification assignments. The two most critical uncertainties, as luck would have it, are for the two modes most critical in model matching: the lowest ℓ modes. The $k = 1$ mode seen in the X2N88 data set has two combinations: plus and minus the $k = 10$ mode. There are no other combinations with these modes; we don’t see them in any other year, and their amplitudes are all quite similar, thus it is impossible with this data to determine which mode is not a combination mode. The most likely choice is that we are seeing the $k = 1$ mode at 110 s and its sum and difference with the $k = 10$ mode. However, we could also be seeing the $k = 1$ mode at 134 s with two sums with the

TABLE 3
OBSERVED PERIODS USED IN
FIGURE 5

k	Period (s)
1 ^a	110
2 ^b	177
3.....	237
4.....	284
5.....	355
6.....	400
8.....	500
9.....	552
10.....	610
11.....	649
12.....	678
13.....	730
14.....	771
15.....	809
16.....	860
17.....	894
18.....	915
??.....	1147
??.....	1240

NOTE.—The k assignments assume all the modes are $\ell = 1$.

^a This mode has a sum and difference combination with the $k = 10$ mode, thus the “real” noncombination mode is either 110 s as shown here, or 134 s.

^b The identity of this mode is questionable. There is excess power in this region, but isolating it to a particular frequency is difficult. It should not be a strong constraint in model-fitting attempts.

$k = 10$ mode. It is unlikely, given the preference for observable sums over differences, that both the 110 s and 134 s are differences with the higher frequency $k = 1$ mode at 93 s.

The $k = 2$ mode identification seen in the 1989 September data set is also uncertain; this time not because of the presence of combinations, but because of the lack of them. This mode is of extremely low amplitude and is not well resolved in the FT. Because of the very high-quality data in this data set, the power seen in the region is probably significant, but we cannot say for certain where the mode is or even whether it is stable over the course of the run. Like the $k = 1$ mode, we don’t see this mode in any other data set. Placing the mode at the highest peak in the region and identifying it as $k = 2$ fits in well with the expected mode pattern, but is highly uncertain.

The X2N88 data contain a messy region of excess power near 2105 μHz , its largest amplitude component. We also see a series of three combination sums of this region (and the 2105 μHz peak) with the large-amplitude $k = 10$ mode. One of either the 2105 μHz peak, or its sums with the $k = 10$ mode, therefore, must be a real oscillation mode, but we cannot decide which it is. No matter which mode it is, however, it does not appear to fit in well with the established pattern of $\ell = 1$ modes and their associated period spacings.

In the 1989 September data, we see two modes at 1986 and 2020 μHz , near what we have been calling the $k = 8$ region, but also significantly different from the power seen there in other years. As seen in the next section, this $k = 8$

mode shows strange multiplet structure and the modes seen here could be some artifact of that. Or, they could be something else entirely; we cannot yet say.

The 1989 September data contain a mode at 2747 μHz and its sum with the 1986 μHz mode. The 2747 μHz mode is about 3 times larger in amplitude than the sum mode, and thus is likely the noncombination mode, but we have no other evidence to support this. Neither mode fits in well with our $\ell = 1$ spacings.

We suspect, therefore, that we do have some non- $(\ell = 1)$ modes in our data, but the lack of repeatability and consistently low amplitude make it difficult to say with certainty. If we accept the $\ell = 1$ assignments for the $k = 1$, $k = 2$, and perhaps even the $k = 8$ modes (1986 and 2020 μHz) of 1989 September, then we have only two modes, the 2105 μHz group of X2N88 and the 2747 μHz pair of 1989 September to explain some other way or with some other ℓ .

6. MULTIPLETS

While we have uncovered strong suggestions for the non-combination modes being all $\ell = 1$, we would like additional proof. Ordinarily, rotational splitting of different m values for a given ℓ and k is a valuable aid in assigning ℓ values. Unfortunately, we do not find many multiplets in this data set. Those that are present do not behave quite as theory predicts. Since a good picture is often worth a few pages of text, we have schematically plotted in Figure 4 the resolved multiplets. This time, the height of each arrow is proportional to the amplitude of the mode (although the scale changes for each multiplet series), and the shorter line segments are not real modes but simply represent the average period of the two flanking modes and are meant to suggest the location of the presumed missing $m = 0$ mode.

We only see identical spacings twice within a given data set. In the X2N88 data, the 500 s and 615 s multiplets both have an $\approx 8.5 \mu\text{Hz}$ spacing. In the 1993 September data, the 400 s and 612 s multiplets both have an $\approx 4.7 \mu\text{Hz}$ spacing. The 400 s multiplet always has the smaller spacing; the 500 s multiplet has the larger; and the 600 s modes alternately fall into both camps. Also note the 400 s multiplet spacing is not constant, but varies (perhaps periodically) with time. All

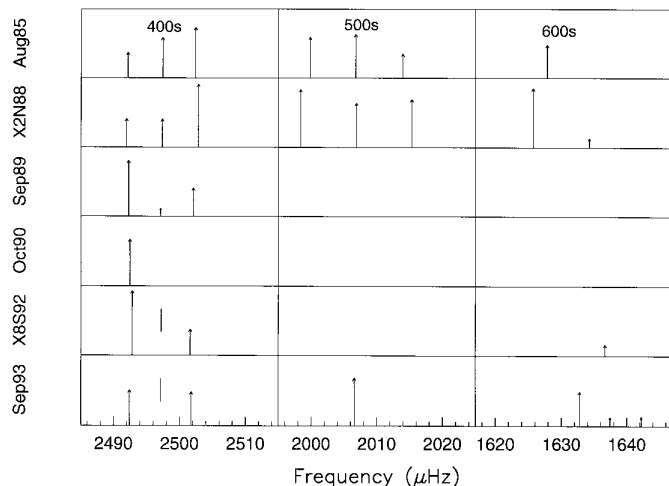


FIG. 4.—Schematic plot of all the major observed multiplets. The short line segments are not real modes, but show the average period of the two flanking modes.

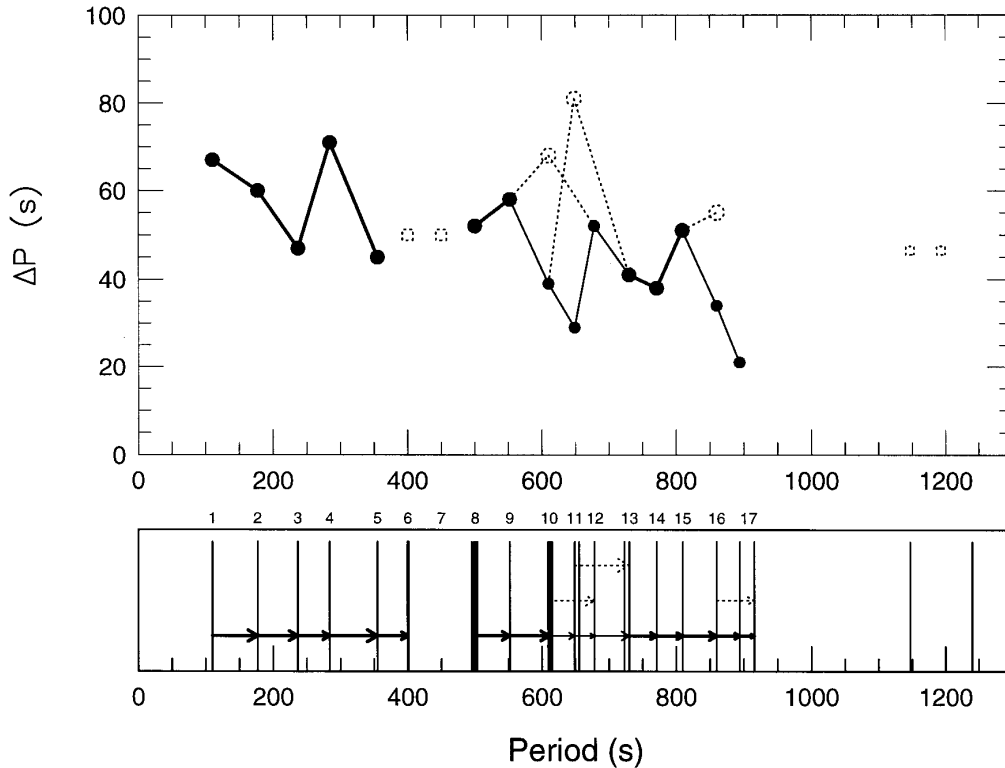
these results are quite interesting, and likely to be clues to the complicated structures in this star, but seem to be largely irrelevant to the overall mode picture. That is not to say there is no information in these changes, however; they may very well be understood by some nonlinear effects such as those discussed by Buchler, Goupil, & Serre (1995). We have only recently begun to acquire the kind of data that could comfortably test such theories. The unfortunate thing here is they do not directly yield information about the ℓ value of our modes, but seem to be even more mysterious if we invoke multiple ℓ 's than if we don't. Thus they support, but do not demand, our $\ell = 1$ model.

7. ANALYSIS

We have now discovered a fairly regular pattern of recurring modes in the power spectra of G29–38 and have suggested they may all form a pattern of successive- k , $\ell = 1$ g -modes. Going just this far is a very important step to uncovering the asteroseismological secrets hidden inside these stars; we never before knew if the modes we were seeing were sustained, normal modes of oscillation or something much more fleeting and chaotic. This is just the first step, however. What remains now is to explore models of DAVs in attempts to tune the input physics to the observed set of frequencies. Such modeling work is a large task and is best allotted a separate work for the detailed, careful analysis and discussion that must inevitably occur. However, here we can address the direction such an effort might take. We do not intend these results to be concrete, but they should help point the modeling investigation in a productive direction.

The goals of the detailed investigation will, of course, be to constrain or determine the mass and internal structure of G29–38. The asteroseismologically determined estimates of both the total stellar and hydrogen layer masses will be particularly important in helping to both calibrate the asteroseismological methods with other mass determinations and check models of white dwarf formation and evolution that set limits on the amount of hydrogen in the DAVs. We also want to see how G29–38 fits in with the other DAVs, both the hot and cool ones. Does it fit the period structure of the hot DAVs found by Clemens (1993, 1994), and does the period spectra of G29–38 look like that of the other cool DAVs, to the extent we can tell? We must defer the full answers to these questions to papers now in progress (however, see Kleinman 1995; Dolez & Kleinman 1997), but will address some of the key issues in a preliminary way here.

If this observed set of modes is a set of single- ℓ pulsations, then the mean period is an indicator of mass and the deviations from the mean describe the layered internal structure of the star. Using forward differences (thus defining ΔP), we have plotted in Figure 5 a ΔP versus P , or period spacing, diagram for these data. With the possible exception of the two modes near $k = 17$, there is no reason to suspect any of these modes are a different ℓ (we later treat these two $k = 17$ modes as $k = 17$ and $k = 18$). Based on the evidence already discussed and previous asteroseismology from WET observations and the work of Clemens with the hot DAVs, it seems unlikely that the majority of the modes are anything other than $\ell = 1$. However, since it is possible we have inadvertently included a mode or two of different ℓ into our identifications, we have plotted some likely alternatives to the ($\ell = 1$)-only model by dotted lines and circles. Where we

FIG. 5.—Observed ΔP vs. P diagram for G29–38

have plotted such alternatives, the only $\ell = 1$ interpretation is plotted with thinner lines and slightly smaller filled circles. The dotted squares represent the average spacing for two modes with an assumed missing mode between them. The bottom panel of the plot is an enlarged plot of the sum row of Figure 2 with arrows showing which modes were used to calculate the differences shown above it. Above this box are $\ell = 1$ k assignments. Each point has an additional uncertainty of a few seconds since we cannot be certain of the m values. In the worst case, the shift can be as much as 14 s for periods near 900 s, and 3 s for periods around 400 s, assuming the largest splitting of $8.5 \mu\text{Hz}$. With the smaller $4.7 \mu\text{Hz}$ splitting, the worst case is about 8 s. Table 3 has a list of the periods used in this diagram (minus multiplets and repeated modes) along with the k assignment in the only $\ell = 1$ model.

Current published models (Bradley 1993, 1996) do not do a very good job of fitting this diagram, but we are encouraged by this as it means there is something we can learn from new modeling efforts. What is different about this diagram is the trend, or perhaps sudden change, to lower period spacing with higher period. This trend could be revealing physics unaccounted for in the model star, or it could mean some of these later modes are not $\ell = 1$, as some of the alternative identifications plotted in Figure 5 suggest. Taking the dotted-line path, this trend effectively disappears, but we have to come up with new assignments for the skipped-over modes. Bradley & Kleinman (1997) have shown, however, that they can get a reasonable DA model to match the observed modes assuming mostly $\ell = 1$.

Based on the ($\ell = 1$)-only interpretation of the observed modes, we calculate a mean period spacing, P_0 , of 47 ± 12 s. This value can increase by a few (3–4) seconds, with the standard deviation decreasing an almost equal amount, if

we take some of the alternative identifications. For now, we will work with the 47 s spacing, determined by assuming *all* the modes are $\ell = 1$ and have the k assignments made earlier. (We have here called the two modes near $k = 17$, $k = 17$ and $k = 18$.)

Using models of Bradley (1996) with a hydrogen layer mass of $1.0 \times 10^{-4} M_*$, consistent with the results of Clemens (1993, 1994) and a temperature of 11,820 K from Bergeron et al. (1995), we have found that this period spacing corresponds to a mass of roughly $0.60 M_\odot$, quite in line with the mean observed white dwarf mass. For this comparison, we used the 11,700 K, $0.6 M_\odot$, standard model with $1.0 \times 10^{-4} M_*$ hydrogen layer and helium layer of $1.0 \times 10^{-2} M_*$, of Bradley (1996) with its mean $\ell = 1$ period spacing (determined from $k = 1$ to $k = 15$) of 47 ± 14 s. Unfortunately, this particular model does not match the individual modes very well, but it helps to establish that the observed period spacing is in the correct range for a reasonable choice of parameters and to note that the standard deviations of the model spacings and our observed spacing are similar.

The mean period spacing is mainly a function of overall stellar mass. The hydrogen layer mass, however, also has an effect, and once we allow it to be a free parameter, we must consider its effects when determining a model asteroseismological fit. If we have another mass measurement, we can fix the overall stellar mass and just vary the hydrogen layer mass to match the observed mean period spacing. The most recent G29–38 mass estimate is from Bergeron et al. (1995). They derive a value near $0.69 M_\odot$. We can fit this mass with our P_0 if we use a $10^{-10} M_*$ hydrogen layer mass (Bradley 1993), although once again, the detailed mode list doesn't match very well.

The most critical mismatch of the above-mentioned models to our list of modes is the $k = 1$ and $k = 2$ modes.

The $0.6 M_{\odot}$ model, for example, has its $k = 1, \ell = 1$ mode at 145 s; the $0.7 M_{\odot}$ model has its $k = 1, \ell = 1$ mode at 210 s. Our labeled $k = 1$ and $k = 2$ modes are at 110 s and 177 s, respectively. There is clearly a mismatch here. The observed $k = 1$ and $k = 2$ modes are certainly the lowest amplitude of the other modes, and therefore more prone to uncertainty, and could possibly be spurious. The case against this, however, is fairly strong, as all the frequencies identified with lower amplitudes than these turned out to be linear combination frequencies; hence their amplitudes are indeed significant. It could also be that these modes are part of unidentified combinations, but there is as yet no evidence for this. It would be nice to see these modes appear again in additional (perhaps archival) data to help answer these questions. Given the ambiguities in the identification of these two modes already discussed, modeling efforts will have to be very careful and rigorous with all the possibilities here.

There is one thing we can say with a much greater confidence: the identified set of noncombination peaks are *not* predominantly $\ell = 2$ modes. Such a spacing with $\ell = 2$ modes implies a stellar mass near $0.2M_{*}$, well out of the range of all previous mass estimates. The majority of the modes must be $\ell = 1$.

Preliminary results (Kleinman 1995; Dolez & Kleinman 1997) show that where modes have been identified in other cool DAVs (from a slightly less comprehensive data set than that presented here), there are usually modes in G29–38 as well. This result extends that of Clemens to include the cooler DAVs and will be published in a future paper. If we follow the same line of reasoning as Clemens, this uniformity also suggests that we have identified predominantly $\ell = 1$ modes.

8. CONCLUSIONS

After many years of searching, we finally have a DAV, G29–38, with enough observed modes to make a detailed asteroseismological analysis possible. With the extensive, 10 yr data set presented here, we have separated the linear combination frequencies from the normal modes that recur in the star's Fourier spectrum. We have uncovered a discrete set of modes from 110 to 1193 s with only a few gaps. We present evidence to support the assertion that these modes are predominantly $\ell = 1$ pulsations. There have never been so many modes in a DAV offered for analysis; we therefore expect surprises. Preliminary modeling efforts do indicate we can match these modes with current models, but so far the matches are not quite as close as we would prefer. These efforts are only preliminary as we have not yet attempted a systematic search of parameter space to fit these observations.

Depending on the exact value of P_0 , the period spacing, and the mass of the hydrogen layer, there may be a discrepancy between the asteroseismological mass and other measurements. The solution to this potential disagreement is as yet unknown, but perhaps more careful modeling efforts will guide us to the answer. Are our mode identifications incorrect, are the models lacking, or is G29–38's behavior affecting the other mass-determination methods, biasing them to an incorrect answer? G29–38's infrared excess, however, as it seemed to be completely independent to the presentation up to this point, remains undiscussed since § 1. Clearly something strange is happening to this star and until we definitively tie down the cause of the infrared

excess, we cannot rule out its possible effects on the pulsations. We are encouraged, however, that B. Zuckerman (1997, private communication) reports that G29–38's IR excess remains unique among the DAVs and that so far, G29–38's pulsation spectrum looks similar to other cool DAVs. An intriguing possibility, however, involves the effect of the large-amplitude pulsations on an H layer close to the nuclear-burning limit. Could this provide the source for both the pulsation instabilities and the IR excess? Koester et al. (1997) suggest not. They report atmospheric detection of heavy elements on the surface of G29–38, consistent with an increased accretion rate from surrounding circumstellar material, perhaps settling the mystery of G29–38's infrared excess.

To help address these questions, we have obtained data on many of the other cool DA pulsators. Preliminary results do not yet address the mass problem (as not enough modes have been identified), but the modes we have seen all appear nearly identical to those in G29–38. This result, when added to Clemens's earlier work on the hotter DAVs, really says the DA's are a very homogeneous class. Therefore, given this set of modes observed in G29–38, it is extremely unlikely that they are anything but $\ell = 1$ pulsations such as have been found in the hotter DAVs. To summarize in broad terms, then, the evidence presented here for a set of $\ell = 1$ modes with a near 47 s spacing in G29–38 is the following:

1. There is a fairly regular ≈ 47 s period spacing observed. This value fits well in the range expected for stars with masses between 0.5 and $0.7 M_{\odot}$.
2. The mean period spacing is too high to be $\ell = 2$ and maintain a reasonable mass for G29–38.
3. When we see multiplets, we see only triplets, consistent with only $\ell = 1$ rotationally split modes.
4. The cool DAVs as a class share many common modes that appear to overlap those of the hotter DAVs that have already been suggested to be $\ell = 1$ modes (Kleinman 1995; Dolez & Kleinman 1997).

If we are going to label these modes as something other than $\ell = 1$ g -modes, we have to explain these four observations as coincidences. One accidental agreement is relatively easy to dismiss; four are much more difficult. There is no easy way to explain the majority of these modes as anything *but* $\ell = 1$.

The suggestion of global uniformity in the DA stars is so profound, we must look at it more closely. In particular, we must direct our efforts at determining both the stellar and hydrogen layer masses. We are now continuing to observe other DA's to determine the extent of their homogeneity. In 1996 February, the WET targeted the cool DAV, HL Tau 76. We hope data from this run, plus previous single-site runs, will uncover a similarly rich pulsation spectrum as we found here. Hopefully, the results from these observations will help guide us to some of the answers we posed earlier. These results should also help address the source of our model-fitting problems, should they remain after a more detailed attempt.

No matter what the numerical results of future modeling are, we have now made the necessary first step for their analysis: we have shown the cool DAVs are normal-mode pulsators whose stable modes reappear in precise places in the power spectra, amidst a veritable forest of combination modes. We have taken a star whose power spectra seemed

unsolvable, rapidly varying, and incapable of providing the kinds of clues needed for an asteroseismological analysis, and extracted these very clues. We must now not only carefully explore model space to match these observations, but obtain similar data on other stars similar to G29–38 so we can begin to determine which conflicts between star and model belong only to G29–38 and which belong to the entire group of stars and, therefore, to our understanding of the general physics that we put into the models. An increased understanding of the physical nature and evolution of the white dwarfs and the chance to calibrate more

accurately the white dwarf cooling sequence, and hence the age of the local galactic disk, await only models to fit to these and future observations.

This work was supported in part by NSF Grants AST 85-52457, AST 86-00507, AST 90-3978, AST 90-14655, AST 92-7988, AST 93-14803, INT-93-14820, and National Committee for Scientific Research grant 2-2109-91-02 (Poland). G. F. wishes to acknowledge the support of the NSREC of Canada and that of the fund FCAR (Quebec).

REFERENCES

- Barnbaum, C., & Zuckerman, B. 1992, *ApJ*, 396, L31
 Bergeron, P., et al. 1995, *ApJ*, 449, 258
 Bradley, P. A. 1993, Ph.D. thesis, Univ. Texas, Austin
 ———. 1996, *ApJ*, 468, 350
 ———. 1998, *ApJ*, submitted
 Bradley, P. A., & Kleinman, S. J. 1997, in *European White Dwarf Workshop, White Dwarfs*, ed. J. Isern, M. Hernanz, & E. Garcia-Berro (Dordrecht: Kluwer), 445
 Brassard, P., Fontaine, G., Wesemael, F., & Hansen, C. J. 1992, *ApJS*, 80, 369
 Breger, M. 1995, *Delta Scuti Newsletter* (Univ. Vienna), 9, 14
 Brown, T. M., & Gilliland, R. L. 1994, *ARA&A*, 32, 37
 Buchler, J. R., Goupil, M.-J., & Serre, T. 1995, *A&A*, 296, 405
 Clemens, J. C. 1993, *Baltic Astron.*, 2, 407
 ———. 1994, Ph.D. thesis, Univ. Texas, Austin
 Dolez, N., & Kleinman, S. J. 1997, in *European White Dwarf Workshop, White Dwarfs*, ed. J. Isern, M. Hernanz, & E. Garcia-Berro (Dordrecht: Kluwer), 437
 Fontaine, G., Brassard, P., Wesemael, F., & Tassoul, M. 1994, *ApJ*, 428, L61
 Fontaine, G., & Wesemael, F. 1997, in *European White Dwarf Workshop, White Dwarfs*, ed. J. Isern, M. Hernanz, & E. Garcia-Berro (Dordrecht: Kluwer), 173
 Kepler, S. O. 1993, *Baltic Astron.*, 2, 444
 Kleinman, S. J. 1995, Ph.D. thesis, Univ. Texas, Austin
 Kleinman, S. J., Nather, R. E., & Phillips, T. 1996, *PASP*, 108, 356
 Kleinman, S. J., et al. 1994, *ApJ*, 436, 875
 Koester, D., Provencal, J., & Shipman, H. 1997, *A&A*, 320, L57
 Liebert, J., Dahn, C. C., & Monet, D. G. 1988, *ApJ*, 332, 891
 McGraw, J. T., & Robinson, E. L. 1975, *ApJ*, 200, 189
 Nather, R. E., Winget, D. E., Clemens, J. C., Hansen, C. J., & Hine, B. P. 1990, *ApJ*, 361, 309
 Robinson, E. L., et al. 1995, *ApJ*, 438, 908
 Shulov, O. S., & Kopatskaya, E. N. 1974, *Astrofizika*, 10, 117
 Unno, W., Osaki, Y., Ando, H., Saio, H., & Shibahashi, H. 1989, *Nonradial Oscillations of Stars* (2d ed.; Tokyo: Univ. Tokyo Press)
 Winget, D. E., Van Horn, H. M., & Hansen, C. J. 1981, *ApJ*, 245, L33
 Winget, D. E., Hansen, C. J., Liebert, J., Van Horn, H. M., Fontaine, G., Nather, R. E., Kepler, S. O., & Lamb, D. Q. 1987, *ApJ*, 315, L77
 Winget, D. E., et al. 1990, *ApJ*, 357, 630
 ———. 1991, *ApJ*, 378, 326
 ———. 1994, *ApJ*, 430, 839
 Zuckerman, B., & Becklin, E. E. 1987, *Nature*, 330, 138
 Zuckerman, B. 1993, in *ASP Conf. Ser. 36, Planets Around Pulsars*, ed. J. A. Phillips, J. E. Thorsett, & S. R. Kulkarni (San Francisco: ASP), 303